Available online at www.sciencedirect.com
SCIENCE DIRECT
Journal of Molecular Catalysis A: Chemical 254 (2006) 145–154
JOURNAL OF MOLECULAR CATALYSIS A: CHEMICAL
www.elsevier.com/locate/molcata

Experimental and DFT investigation of the 1-octene metathesis reaction mechanism with the Grubbs 1 precatalyst

M. Jordaan, P. van Helden, C.G.C.E. van Sittert, H.C.M. Vosloo *

School of Chemistry, North-West University (Potchefstroom Campus), 2520 Potchefstroom, South Africa

Available online 24 April 2006

Abstract

Using density functional theory the metathesis reactions of 1-octene in the presence of Grubbs 1 [$RuCl_2(PCy_3)_2$(=CHPh)] is investigated. At the GGA-PW91/DNP level, the complete geometry optimization and the activation energy of various activation steps and catalytic cycles in the dissociative mechanism are performed. The formation of the catalytically active heptylidene species is kinetically and thermodynamically favoured, while the formation of *trans*-tetradecene is thermodynamically favoured. The computational results are in agreement with the experimental results obtained with NMR and GC/MSD experiments. Grubbs 1 is active for the metathesis of 1-octene at 25 °C yielding *trans*-7-tetradecene as the major product. The formation of by-products, i.e. styrene isomers and PCy_3, is consistent with the dissociative metal carbene mechanism. The rapid formation of the heptylidene derivative of Grubbs 1 is observed by in situ NMR.

Keywords: Alkene metathesis; 1-Octene; Mechanism; Grubbs 1; Molecular modelling; DFT

1. Introduction

Alkene metathesis is extensively used in catalysis and synthesis for the formation of carbon–carbon double bonds [1–5]. During this catalytic reaction, linear alkenes are transformed into homologs of shorter and longer carbon chains. The ruthenium carbene complexes developed by the Grubbs group, $RuCl_2LL'$(=CHPh) (L, L′ = PCy_3 (**1**) and L = PCy_3, L′ = NHC (**2**)), are of interest because of their high metathesis activity and tolerance towards polar functional groups [6,7]. The catalytic activity and selectivity of the $RuCl_2(PCy_3)_2$(=CHPh) (**1**) precatalyst towards the primary metathesis products, in the 1-octene metathesis reaction, was reported to be high even at an alkene/Ru molar ratio = 10,000 [6,7]. Replacement of the phosphine ligand(s) by *N*-heterocyclic carbene ligands improved the lifetime and reactivity of the metal carbene complex even further [8]. This is due to the bulkiness and increased basicity of the NHC ligand compared to PCy_3 [9].

The Hérisson-Chauvin metal carbene mechanism is the generally accepted mechanism for the alkene metathesis reaction (Scheme 1) [10]. The mechanism consists of successive [2 + 2] cycloadditions followed by cycloreversions. This involves the coordination of the alkene to the metal centre to form a π-complex followed by the formation of a metallacyclobutane intermediate, which in turn can revert to a new π-complex to yield the products after dissociation.

Although many aspects of the alkene metathesis mechanism in the presence of **1** were elucidated by various techniques including kinetic measurements [11–13], there are still aspects that need to be investigated. This includes determining the species that is the most active in the metathesis reaction as well as elucidating the mechanism when the benzylidene and not the methylidene are used as precatalyst. The alkene metathesis reaction with Ru–carbene complexes has been studied by molecular modelling mainly using simple substrates and simplified ligands. Adlhart and Chen [14] have summarized the mechanistic pathways, which can be divided into two main categories, i.e. an associative and dissociative mechanism. Recent studies indicate that the dissociative mechanism, which is initiated by the dissociation of a phosphine ligand from $RuX_2(PR_3)_2$(=CHR) to form a 14-electron species, is preferred [13–15]. Chen and co-workers [16] confirmed this by the identification of the 14-electron species by gas-phase mass spectrometry. The rate of phosphine dissociation and initiation of the alkene metathesis reaction by $RuX_2L(PR_3)$(=CHR) type precatalysts have been investigated theoretically and experimentally by Sanford et al. [13].

In this study we report on the mechanism of 1-octene metathesis with the first generation Grubbs complex or Grubbs 1 (**1**).

* Corresponding author. Tel.: +27 18 299 2358; fax: +27 18 299 2350.
E-mail address: chehcmv@puk.ac.za (H.C.M. Vosloo).

1381-1169/$ – see front matter © 2006 Elsevier B.V. All rights reserved.
doi:10.1016/j.molcata.2006.03.022

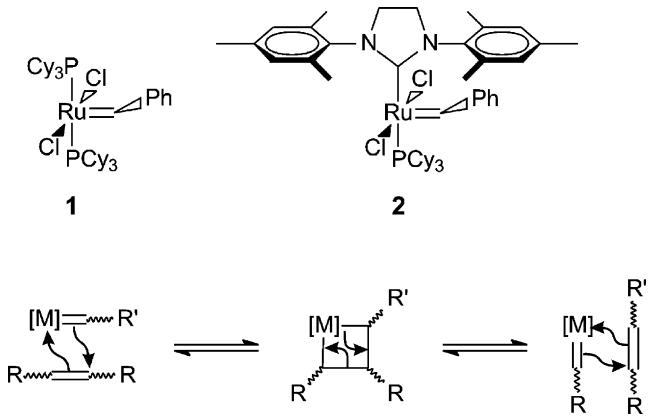

Scheme 1. Hérisson-Chauvin metal carbene mechanism.

A conceptual model of the complete mechanism is presented. The results from our quantum-mechanical calculations are used to compare the ^{1}H NMR and other experimental results with the proposed steps of the catalytic cycle and to gain insight into the complete productive mechanism of the 1-octene metathesis reaction with **1**. The modelling results indicate that the formation of the heptylidene is kinetically and thermodynamically more favourable than the formation of the methylidene. The formation and interaction of the carbene active species using ^{1}H NMR is shown. The mechanism is further supported by the formation of by-products, i.e. styrene, 1-phenyl-1-octene isomers and PCy_3.

2. Experimental section

2.1. Materials and methods

1-Octene (Aldrich) was passed through a column of basic alumina and stored on molecular sieves (4 Å) under nitrogen. Chlorobenzene (Merck) was dried with calcium hydride and stored under nitrogen. $RuCl_2(PCy_3)_2$(=CHPh) 1 (Fluka) were used as received.

The metathesis reactions were carried out in GC autosampler vials (3 mL) and continuously analyzed on an Agilent 6890 gas chromatograph equipped with an Agilent 7683 autoinjector, HP-5 capillary column (30 m × 320 μm × 0.25 μm) and a flame ionization detector (FID). The following instrument conditions were used: inlet temperature of 200 °C, oven programmed from 60 to 130 °C (hold time 16 min) and 130 to 290 °C (hold time 5 min) at 25 °C min^{-1}, N_2 carrier gas with a flow rate of 2 mL min^{-1} at 20 °C and FID temperature of 250 °C. For product verification the reaction mixtures were also analyzed using an Agilent 6890 gas chromatograph equipped with an Agilent 7683 autosampler, HP-5 MS capillary column (30 m × 320 μm × 0.25 μm) and an Agilent 5973 mass selective detector (MSD). The same oven program was used with a 6 min solvent delay and He as carrier gas with a 1 mL min^{-1} flow rate at 20 °C. The ^{1}H NMR spectra were recorded on a Varian Gemini 300 Broadband NMR spectrometer at 300 MHz in deuterated chloroform.

2.2. Metathesis experiments

Metathesis experiments were performed by adding 1-octene (2.5 mL, 1000 mol) to a solution of **1** (13.2 mg, 1 mol) in chlorobenzene (1.25 mL). Chlorobenzene served as solvent and internal standard for quantification of the GC results. The reactions were performed at 25 °C and the progress monitored by GC/FID. Aliquots (0.2 μL) of the reaction mixture were injected at approximately 40 min intervals with the autoinjector. After 3 h the same volume was analyzed by GC/MSD to characterize the mixture. The response factor of an authentic sample of each major alkene component were determined and used in the conversion calculations.

The ^{1}H NMR investigation of the 1-octene metathesis reaction was performed in a NMR tube with 1-octene (0.05 mL, 10 mol) mixed with a solution of **1** (1 mol, 26.2 mg) in $CDCl_3$ (0.75 mL). Spectra were recorded at approximately 10 min intervals.

2.3. Computational details

The quantum-chemical calculations were carried out by density functional theory (DFT) since it usually gives realistic geometries, relative energies and vibrational frequencies for transition metal compounds. All calculations were performed with the DMol^3 DFT code [17] as implemented in Accelrys Materials Studio® 3.2 [18] on 3 GHz Pentium IV computers with 1 GB RAM. The non-local generalized gradient approximation (GGA) functional by Perdew and Wang (PW91) [19] was used for all geometry optimisations. The convergence criteria for these optimisations consisted of threshold values of 2×10^{-5} Ha, 0.004 Ha/Å and 0.005 Å for energy, gradient and displacement convergence, respectively, while a self-consistent field (SCF) density convergence threshold value of 1×10^{-5} Ha was specified. DMol^3 utilizes a basis set of numeric atomic functions, which are exact solutions to the Kohn–Sham equations for the atom [20]. These basis sets are generally more complete than a comparable set of linearly independent Gaussian functions and have been demonstrated to have small basis set superposition errors [20]. In this study a polarized split valence basis set, termed double numeric polarized (DNP) basis set has been used. All geometry optimisations employed highly efficient delocalised internal coordinates [21]. The use of delocalized coordinates significantly reduces the number of geometry optimisation iterations needed to optimise larger molecules compared to the use of traditional Cartesian coordinates.

Some of the geometries optimised were also subjected to full frequency analyses at the same GGA/PW91/DNP level of theory to verify the nature of the stationary points. Equilibrium geometries were characterised by the absence of imaginary frequencies. Preliminary transition state (TS) geometries were obtained by the integrated linear synchronous transit/quadratic synchronous transit (LST/QST) algorithm available in Materials Studio® 3.2. This approach was used before in computational studies in homogeneous trimerisation and metathesis [22]. These preliminary structures were then subjected to full TS optimisations using an eigenvector following algorithm. For selected transition

state geometries confirmation calculations, involving intrinsic reaction path (IRP) calculations, were performed in which the path connecting reagents, TS and products are mapped. The IRP technique used in Materials Studio® 3.2 also corresponds to the intuitive minimum energy pathway (MEP) connecting two structures and is based on the nudged elastic band (NEB) algorithm of Henkelman and Jonsson [23]. The IRP calculations, performed at the same GGA/PW91/DNP level of theory, ensured the direct connection of transition states with the respective reactant and product geometries. All transition structure geometries exhibited only one imaginary frequency in the reaction coordinate. All results were mass balanced for the isolated system in the gas phase. The energy values that are given in the results are the electronic energies at 0 K and therefore only the electronic effects are in consideration in this paper.

3. Results and discussion

3.1. Metathesis of 1-octene using *1*

Alkene isomerisation and metathesis (homo- and cross metathesis) reactions can take place during the metathesis of 1-octene to form a variety of products. The possible reactions 1-octene can undergo in the presence of a metathesis (pre)catalyst are presented in Table 1. Three major groups of products, i.e. primary metathesis products (PMP), isomerisation products (IP) and secondary metathesis products (SMP), are possible. Following the double bond isomerisation of 1-octene to 2-octene secondary cross metathesis between the two alkenes can take place yielding 1-heptene which in turn can undergo the same series of reactions. This gives rise to a cascade of reactions eventually leading to a range of C_2–C_{14} alkene products (SMP).

The catalytic conversion of 1-octene to 7-tetradecene with **1** was performed at room temperature (25 °C) at a 1-octene/Ru molar ratio of 1000. The reaction mixture was continuously monitored by GC/FID to determine the different products that forms during the metathesis of 1-octene; these products were identified by GC/MSD. The homometathesis of 1-octene leads to the formation of two isomers (Fig. 1), *cis*- and *trans*-7-tetradecene, which combined with ethene (not observed) represents the PMP of the reaction. 1-Octene was converted to approximately 22% *trans*- and 9% *cis*-7-tetradecene (approximately 62% PMP) after 300 min (Fig. 2). SMP due to the double bond isomerisation of 1-octene to mainly 2-octene and the subsequent metathesis reactions remain below 5%. This indicates that **1** has a high selectivity towards PMP formation, i.e. 94%. After 3 h the following by-products were also identified in the reaction mixture with the aid of GC/MSD (Fig. 3), i.e. styrene, *cis*- and *trans*-1-phenyl-1-octene (or hexyl styrene), PCy_3 and $OPCy_3$. The presence of PCy_3 in the reaction mixture is consistent with the dissociation step leading to the active 14-electron benzylidene species. Furthermore, the presence of the styrenes is indicative of the formation of ruthenium methylidene and heptylidene species. The different orientation possibilities of coordination of 1-octene to the Grubbs 1 benzylidene metal

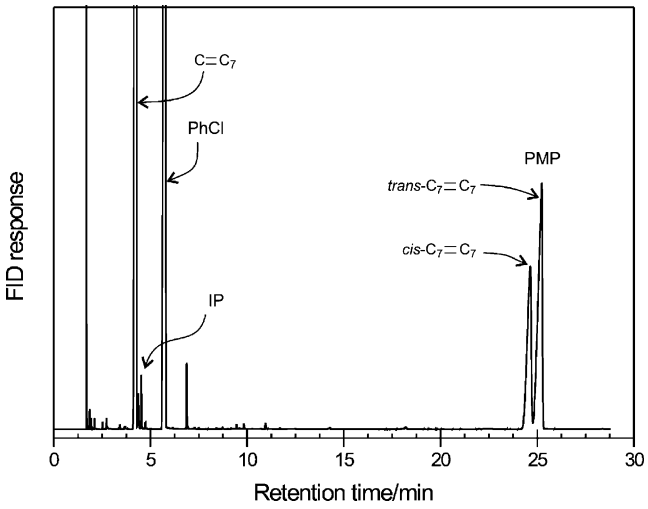

Fig. 1. GC/FID chromatogram of the reaction mixture of 1-octene in the presence of $RuCl_2(PCy_3)_2$(=CHPh) at 25 °C after 1 h (solvent = chlorobenzene, 1-octene/Ru = 1000).

Table 1
Possible reactions of 1-octene in the presence of metathesis catalysts

Reaction	Substrate[a]	Products[a]
Primary metathesis		
Homometathesis[b]	C=C7	C=C + C7=C7 (PMP)[c]
Isomerisation	C=C7	C2=C6 + C3=C5 + C4=C4 (IP)[d]
Secondary metathesis		
Cross metathesis[e]	C=C7 + C2=C6	C2=C7 + C=C6 + C=C2 + C6=C7 (SMP)[f]
Homometathesis[b]	C2=C6	C2=C2 + C6=C6 (SMP)[f]

[a] Hydrogens are omitted and geometrical isomers not shown for simplicity.
[b] Homometathesis refers to the metathesis reaction between the same alkenes.
[c] Primary metathesis products (PMP) refers to the homometathesis products of 1-octene i.e. C_7=C_7 and C=C.
[d] Isomerisation products (IP) refers to the double bond isomerisation reaction of terminal to internal alkenes.
[e] Cross metathesis refers to the metathesis reaction between different alkenes.
[f] Secondary metathesis products (SMP) refers to the metathesis of the isomerisation products of 1-octene.

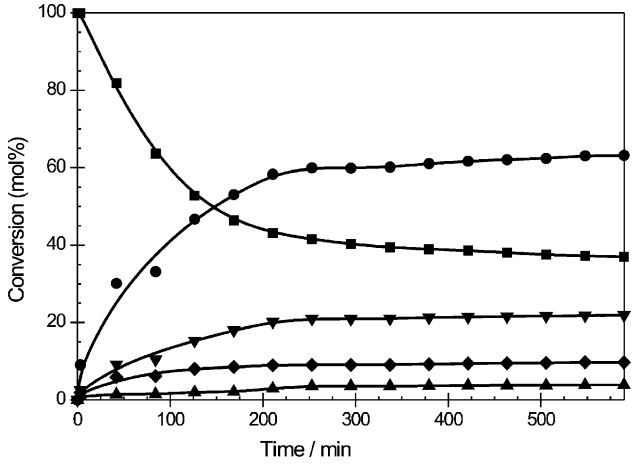

Fig. 2. Reactions of 1-octene in the presence of $RuCl_2(PCy_3)_2$(=CHPh) at 25 °C (solvent = chlorobenzene, 1-octene/Ru = 1000). [■ 1-octene, ● PMP, ▼ *trans*-7-tetradecene, ♦ *cis*-tetradecene, ▲ SMP].

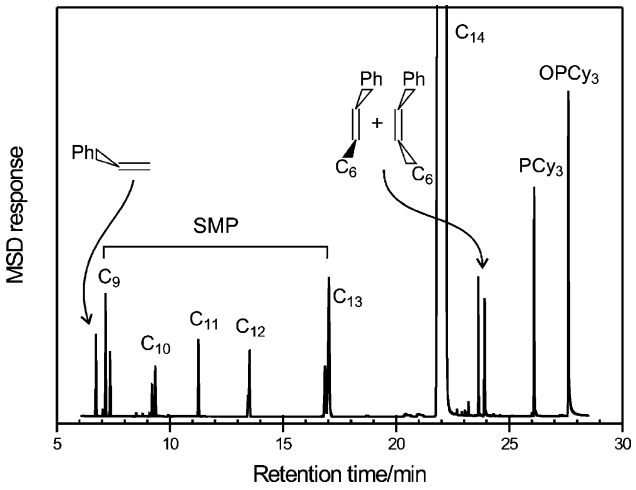

Fig. 3. GC/MSD chromatogram of the reaction mixture of 1-octene in the presence of $RuCl_2(PCy_3)_2(=CHPh)$ at 25 °C after 3 h (solvent = chlorobenzene, 1-octene/Ru = 1000, solvent delay = 6 min, MSD response enlarged).

centre leads to the formation of a heptylidene species with the liberation of styrene or the methylidene species with the liberation of the hexyl styrenes.

We also investigated the metathesis of 1-octene with ^{1}H NMR and the involvement of the three carbene species are clearly illustrated (Fig. 4). The carbene α-H signal of the benzylidene [$RuCl_2(PCy_3)_2(=CHPh)$] appears at δ 20.015 ppm, of the heptylidene [$RuCl_2(PCy_3)_2(=CHC_6H_{13})$] at δ 19.310 ppm and the methylidene [$RuCl_2(PCy_3)_2(=CH_2)$] at δ 18.954 ppm. The shift of the carbene α-H peak of the benzylidene to lower field to produce a doublet and singlet is due to the change in the electronic environment of the ligand attached to the carbene carbon. Due to the fast initiation rate (0.13 ± 0.01/s) [24] of Grubbs 1 during the metathesis reaction, all three carbene signals are already present after 14 min.

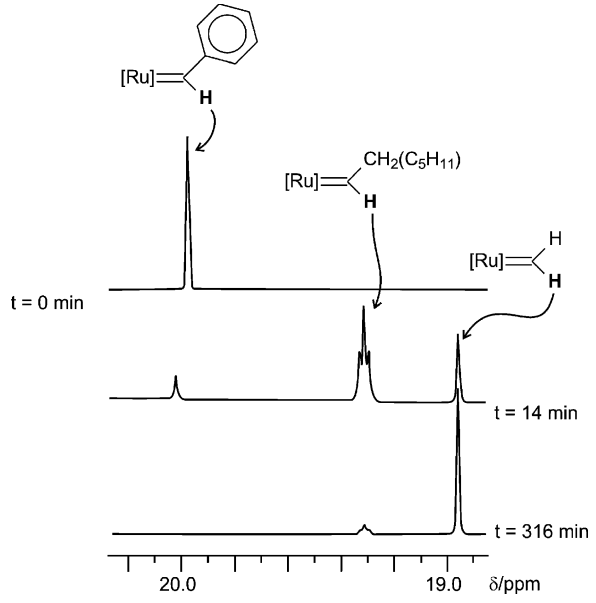

Fig. 4. ^{1}H NMR spectra of the carbene proton region at different time intervals of a 1-octene/$RuCl_2(PCy_3)_2(=CHPh)$ reaction mixture in $CDCl_3$ at 25 °C.

The change over time in the size of the carbene α-H signals of the three carbene species involved in the metathesis of 1-octene is given in Fig. 5. The size of the benzylidene signal gradually decreases (Fig. 5(a)) suggesting the conversion of the benzylidene to the heptylidene and methylidene; after 300 min all of **1** has been converted (see also Fig. 4). The simultaneous decomposition of the benzylidene to some other species cannot be ruled out. The sharp increase to a maximum of the heptylidene signal within 14 min is followed by a gradual decrease as the reaction proceeds (Fig. 5(b)) while the methylidene signal gradually increases to a maximum within 2 h followed by a slow decrease (Fig. 5(c)) possibly due to catalyst decomposition. In the presence of 1-octene it seems as if the benzylidene is rapidly converted to the heptylidene while the formation of the methylidene proceeds at a much slower rate. Ulman and Grubbs [12] also observed that the alkylidene is generally the more reactive compared to the methylidene in the metathesis of alkenes with **1**.

3.2. Model system and notations

Conceptually the productive metathesis of 1-octene in the presence of Grubbs carbene complexes is illustrated in Schemes 2 and 3. This mechanistic model is mainly based on the dissociative mechanism proposed by Grubbs et al. [13,15], modelled by Adlhart and Chen [14] and our experimental results.

The generic labels **A**–**I** are given to the individual ruthenium carbene and derived species involved in the reaction mechanism. The mechanism consists of the initial loss of PCy_3 from **1** (**A**) to yield $RuCl_2(PCy_3)(=CHPh)$ (**B**). The different stereochemical approaches of 1-octene towards the catalytically active species (**B**, **F1**, **F3** and **F4**) leads to four activation steps (**1**–**4** notations in Scheme 2) and six catalytic cycles (**a** and **b** notations in Scheme 3). To identify which step is under consideration, a numerical suffix (**1**–**4**) is associated with the labels **C** to **I** (e.g. **C1**–**F1** represents activation step **1**) and the additional alphabetic suffixes a and b indicates the different catalytic cycles. Transition states are denoted analogously, e.g. **G3a**–**H3a** is the transition state for the conversion of **G3a** to **H3a**.

The mechanism is initiated by the dissociation of a phosphine ligand from the 16-electron benzylidene complex **A** to form the 14-electron active species **B** (Scheme 2). This is followed by activation steps (Scheme 2) and catalytic cycles (Scheme 3) based on the stereochemical approaches of the 1-octene towards the different carbene species. These steps/cycles consist of several successive formal [2 + 2] cycloadditions to form a metallacyclobutane and cycloreversions to form the respective catalytically active species. Before the precatalyst can enter the catalytic cycle, there is an initiation phase (activation) in which the catalyst first has to be converted from the benzylidene complex (**A**) to the methylidene (**F1**, the second activation step will also yield **F1**) or heptylidenes (**F3** and **F4**). This takes place through the coordination of 1-octene to the metal centre of the 14-electron intermediate to form a π-complex, which undergoes a formal [2 + 2] cycloaddition to form a metallacyclobutane ring, which in turn can revert to a new π-complex. The liberation of the alkene from the new π-complex leads to the new catalytically

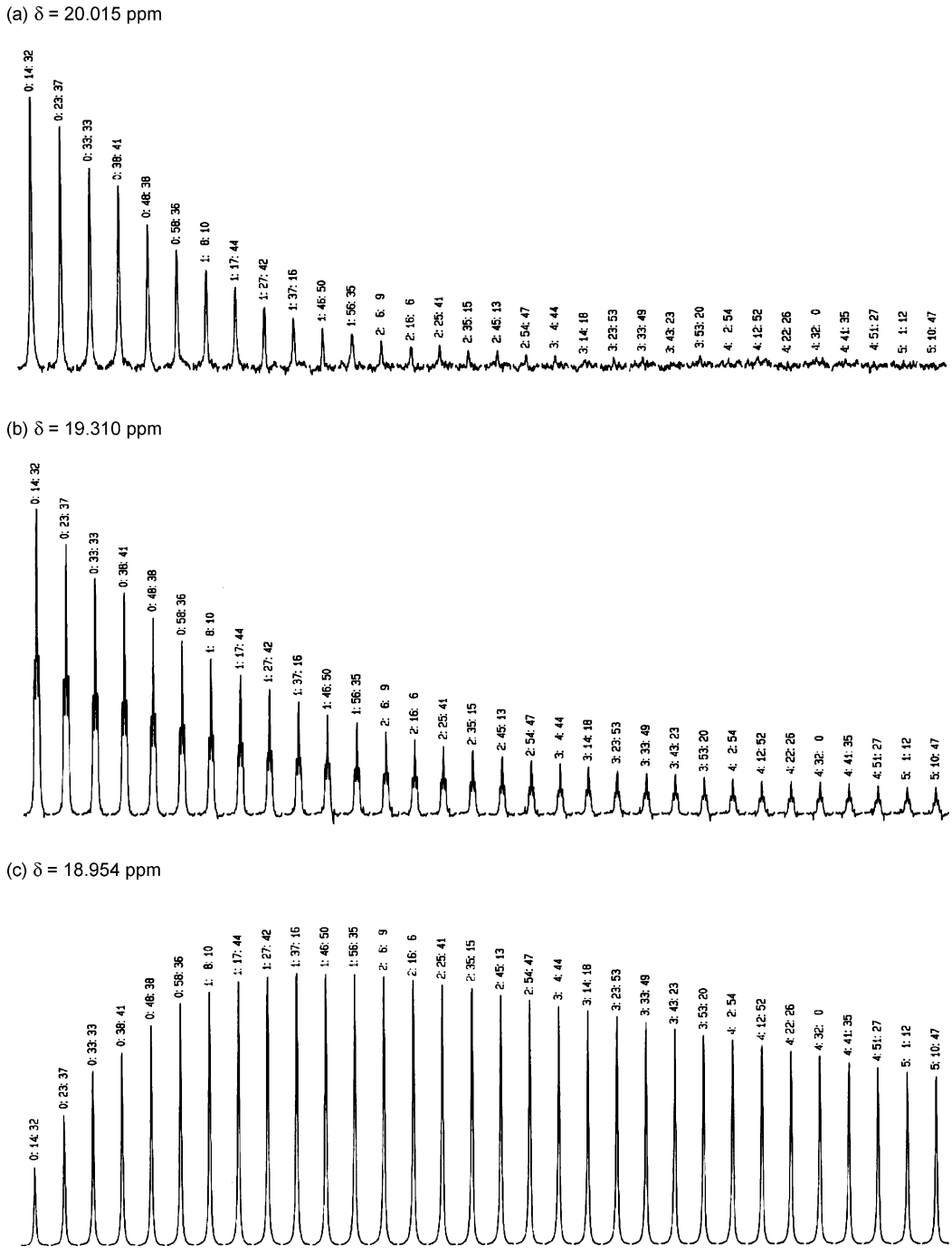

Fig. 5. ^{1}H NMR signals at different time intervals of the carbene α-Hs in a 1-octene/$RuCl_2(PCy_3)_2$(=CHPh) reaction mixture in $CDCl_3$ at 25 °C [(a) Ru=CHPh, (b) Ru=CHC_6H_{13} and (c) Ru=CH_2].

active alkylidene species that enters the catalytic cycle. Activation steps 1 and 2 leads to the formation of the methylidene complex with the liberation of *cis*- and *trans*-1-phenyl-1-octene. In the other two activation steps styrene is liberated to form the heptylidene species with the alkyl chain of the carbene facing out of (**F3**) or into (**F4**) the plane of the paper, depending on the coordination orientation of 1-octene relative to the phenyl ring of the carbene that is facing into the plane. Within the catalytic cycles the heptylidene is converted to the methylidene, which is then again converted back to the heptylidenes until all the 1-octene has been consumed or the catalyst has decomposed. During the conversion of the heptylidene to the methylidene, *cis*- and *trans*-7-tetradecene is formed, while ethene forms when the methylidene is converted to the heptylidene.

3.3. Molecular modelling

Theoretical studies can be of immense use to resolve the effect of ligand coordination and to gain deeper insights into the mechanism of catalytic reactions. There have been a few recent studies

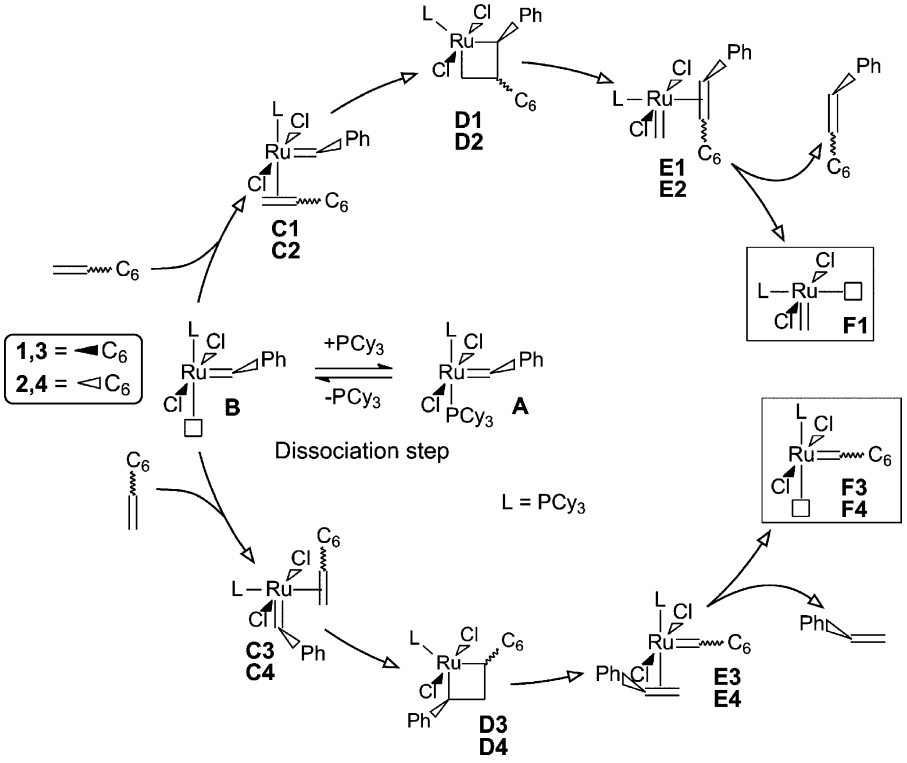

Scheme 2. Dissociation (**A**–**B**) and activation (**B**–**F**) steps in the mechanism of productive 1-octene metathesis using $RuCl_2(PCy_3)_2(=CHPh)$.

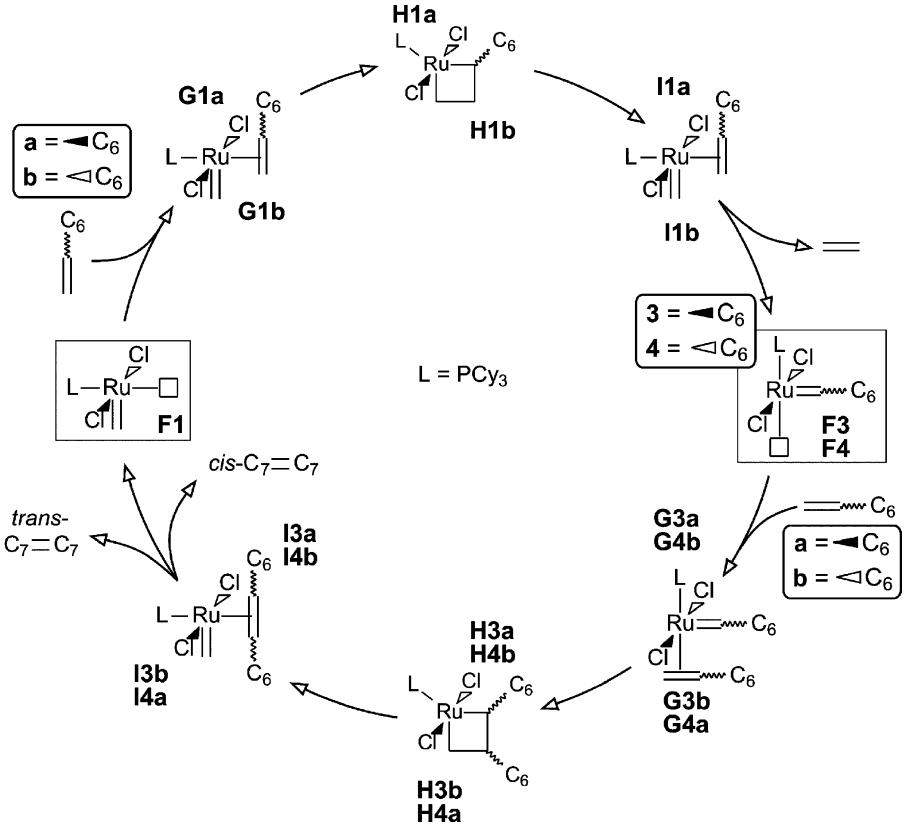

Scheme 3. Catalytic cycles in the mechanism of productive 1-octene metathesis using $RuCl_2(PCy_3)_2(=CHPh)$.

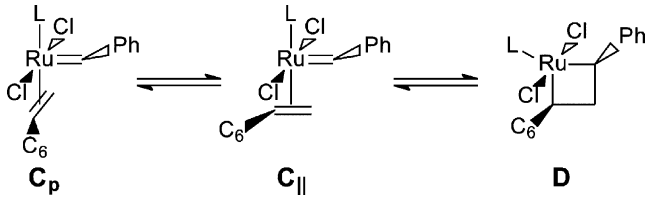

Scheme 4. *Trans* alkene coordination in the dissociative pathway.

that calculated mechanistic parameters or combined experimental work with computational studies on the alkene metathesis mechanism with ruthenium carbenes [13,14,16,25–31]. In these studies the catalytic cycle and ligand dissociation of the methylidene species (**F1**) were extensively explored. In many of these studies use were made of model PR_3 (R = H, Me) ligands and/or ethene as model substrate with the methylidene complex $RuCl_2(PR_3)_2(=CH_2)$ to mainly reduce the computing cost. This leaves room for interpretation concerning the steric and electronic influences of the actual ligands (PCy_3 versus PR_3 (R = H, Me)) and substrates (1-octene versus ethene) with the benzylidene complex (versus methylidene complex) as precatalyst.

The quantum-chemical calculations that we employed in this study were applied to the $RuCl_2(PCy_3)_2(=CHPh)$ complex with a closer focus on the *trans* addition of 1-octene to the catalytically active species. The coordination of the alkene *trans* with respect to the ligand L is the most favourable pathway due to the fact that large phosphines, like PCy_3, has a Tolman cone angle of 170° [32,33] and the position *trans* with respect to the carbene would be avoided due to the strong σ-donor effect of the carbene bond. This is shown to be the case according to the computational studies of Adlhart and Chen [14] (ADF program, BP86 functional) in which the coordination of the alkene *trans* towards L is one of the two most favourable pathways in the catalytic cycle. The coordination of the alkene in the *trans* position can be in two discrete, perpendicular orientations (Scheme 4). In our study the coordination of the alkene parallel to the Cl–Ru–Cl line and perpendicular or orthoganal to the carbene ($\mathbf{C}_P$) was used in the equilibrium geometry calculations of the π-coordination structures (**C**, **E**, **G** and **I**) because it was found to be the energetically favoured geometry. If the alkene coordinates in the $\mathbf{C}_p$ mode (Scheme 3) it has to turn approximately 90° to align with the benzylidene carbene bond ($\mathbf{C}_{II}$ mode) to yield the metallacyclobutane intermediate (**C**–**D**, etc.). The $\mathbf{C}_p$–$\mathbf{C}_{II}$ conversion is currently under investigation. For the sake of simplicity all the π-coordination structures are given in the $\mathbf{C}_{II}$ mode.

For the purpose of this study the global minimum structure obtained from the geometry optimisation (GGA/PW91/DNP) of 1-octene was used with the hexyl chain constrained in further calculations. In this structure the hexyl chain was "straight" and remained so in optimisations of intermediates where the hexyl chain was kept unconstrained to confirm the constrained conformation. The influence of other conformers of 1-octene on the energetics of the reaction pathway was not considered further in this study.

In an attempt to get a better idea of the validity of the computational method we used in this study comparisons are made of key bond lengths and angles of **1**. The calculated bond lengths and angles are compared with crystallographic data reported by Nguyen and Trnka [34] and calculated values obtained by Adlhart and Chen [35] (Table 2). An acceptable correlation is obtained with bond lengths being overestimated and bond angles generally being underestimated in the calculations.

Table 2
Crystallographic and theoretical values of key bond lengths and angles of $RuCl_2(PCy_3)_2(=CHPh)$.

	Exp.[a]	Calculated[b]	Calculated[c]
Bond lengths (Å)			
Ru=C	1.838 (2)	1.878	1.860
$Ru–Cl_{avg}$	2.390 (1)	2.452	2.420
$Ru–P_{avg}$	2.416 (1)	2.490	2.435
Bond angles (°)			
Cl–Ru–Cl	168.21 (2)	160.97	162.4
P(1)–Ru–P(2)	161.90 (2)	163.35	–
Ru=C–R	136.70 (2)	136.04	–

[a] Ref. [34].
[b] DMol[3] GGA/PW91/DNP—full DFT calculation of geometries.
[c] Ref. [35] (ADF BP86—QM/MM calculation of geometries).

We also modelled the activation steps of **1** with ethene to the corresponding metallacyclobutane intermediate and compared our results with the values obtained by other authors (Fig. 6). The electronic energy profile we calculated was for the Grubbs 1 benzylidene system, while the electronic energies obtained by Adlhart and Chen [14] (ADF program, BP86 functional, triple ξ basis set on ruthenium and a polarized double ξ basis set for all other elements) and Burdett et al. [28] (Jaguar 4.1 program, B3LYP hybrid functional, LACVP** basis set) was calculated for the Grubbs 1 methylidene. It has been shown that sterically bulky and electron-donating R groups (e.g. alkyl, Ph) lead to higher initiation rates (phosphine dissociation) because they more effectively promote phosphine dissociation, while small and electronically neutral groups (e.g. H) are less effective at labilizing the phosphine ligand [12]. This is not significantly clear in Fig. 6. The trend for the formation of

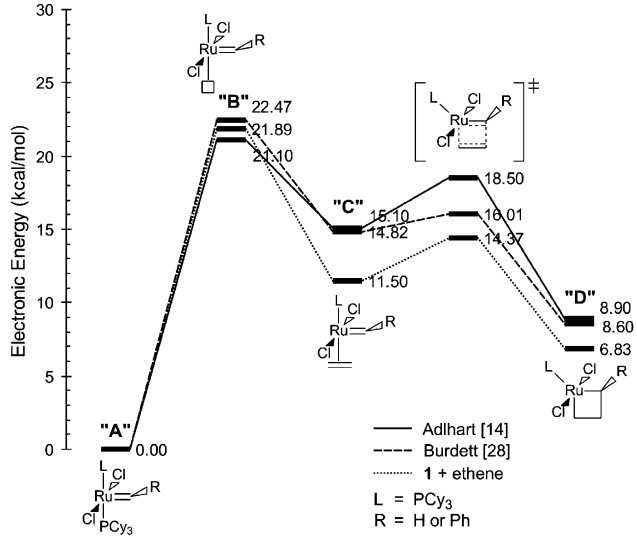

Fig. 6. A comparison of the calculated and literature electronic energy profiles of the activation steps of ethene metathesis using $RuCl_2(PCy_3)_2(=CHR)$.

the metallacyclobutane ring is similar in all three cases, but a more stable 16-electron complex ("**C**") as well as a 14-electron metallacyclobutane ("**D**") is obtained from the benzylidene complex. It was shown that electron-withdrawing phosphine ligands will destabilize the 14-electron metallacyclobutane intermediate ("**D**") relative to the 14-electron carbene species ("**B**") [14]. Therefore the presence of an electron-donating species will have a stabilization effect on these complexes. This explains the catalytic activity of the methylidene but lack of activation by the benzylidene.

The coordination of the substrate to the 14-electron species (**B–C**) is a step that is in competition with the recoordination of the phosphine ligand (**B–A**). In our model there is only one substrate molecule competing with one phosphine, although in a catalytic system with catalyst to substrate ratios of 1:500 or more this competition is statistically favoured towards the substrate. The stoichiometric competition described in our model excludes this statistical competitiveness. The competition can be described by comparing the energy of coordination of the phosphine to the energy of coordination of the substrate by taking the ratio of the respective energy differences. These values are summarized by the ratio $\Delta E_{B-A}/\Delta E_{B-C}$ in Table 3 for the metathesis of 1-octene and ethene with **1**. Generally for Grubbs

Table 3
Comparison of electronic energies of the π-coordination intermediate $RuCl_2(PCy_3)L(=CHPh)$ containing ethene and 1-octene

L	Energy ratios		ΔE_{B-C} (**B–C**) kcal/mol	$\Delta E_o^{\ddagger}$ (**C** to **C–D**) kcal/mol
	$\Delta E_{B-A}/\Delta E_{B-C}$	$\Delta E^{\ddagger}_{o,TS-D}/\Delta E^{\ddagger}_{o,TS-C}$		
Ethene	1.99	0.97	−10.54	7.80
1-Octene	3.69	1.23	−5.70	9.74

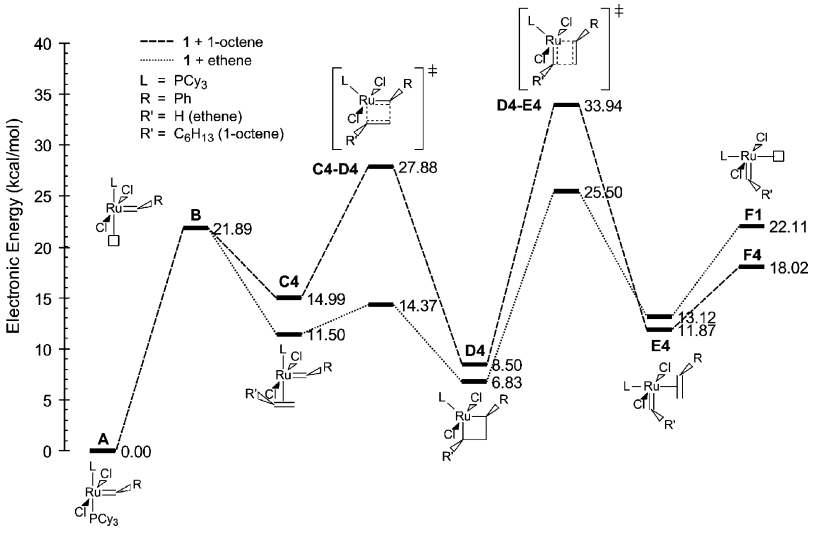

Fig. 7. Electronic energy profiles of the activation steps of the metathesis of ethene and 1-octene using $RuCl_2(PCy_3)_2(=CHPh)$.

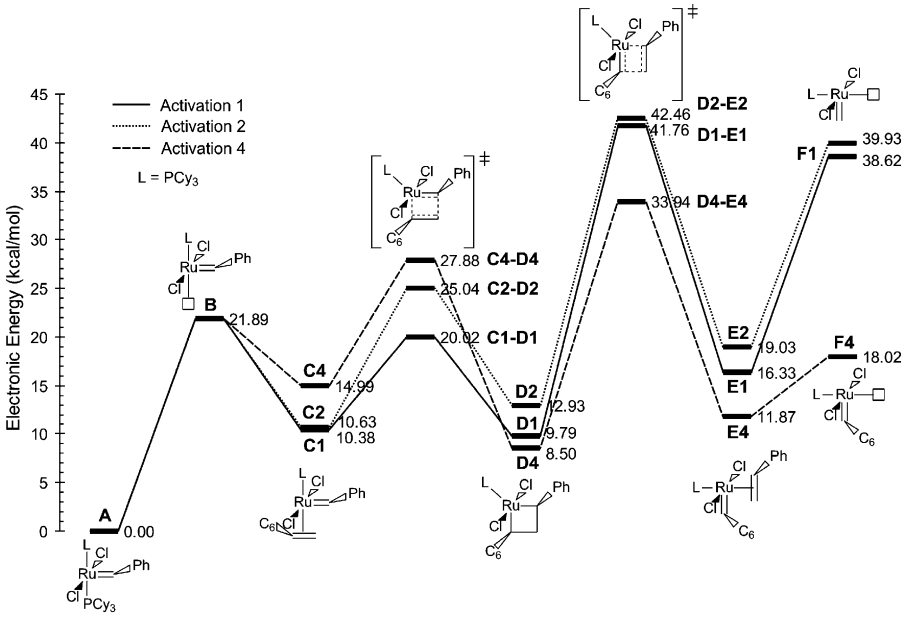

Fig. 8. Electronic energy profiles of the activation steps in the productive 1-octene metathesis using $RuCl_2(PCy_3)_2(=CHPh)$ (**C4–F4** structures only are shown).

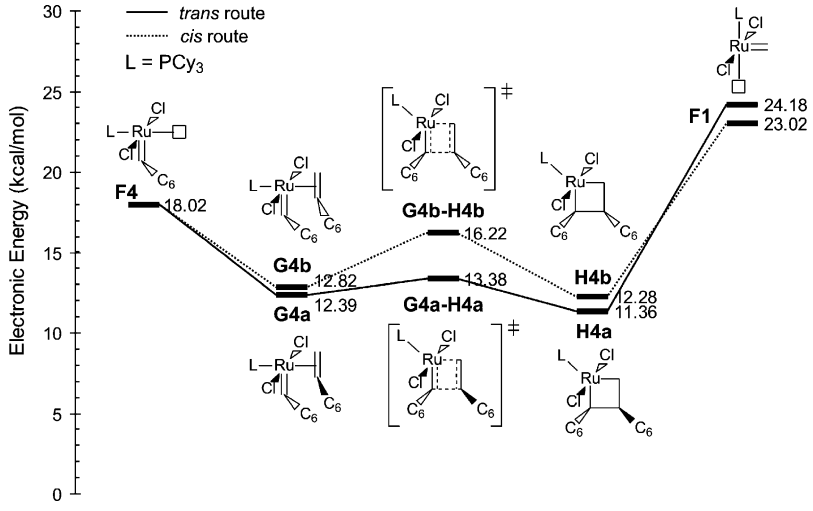

Fig. 9. Electronic energy profile of the *trans* and *cis* routes from the heptylidene **F4** to the methylidene **F1**.

1 (**1**) phosphine recoordination is favoured, while the affinity towards phosphine increases with an increase in the chain length of the substrate.

If the electronic energy profiles of **1** with ethene and 1-octene is compared (Fig. 7) it is clear that the 1-octene does not coordinate as strongly as the ethene to **B** ("**C**"). The electronic energy of activation of "**C**" to "**D**" with ethene is 2.87 kcal/mol while the value with 1-octene is 12.89 kcal/mol. Adlhart and Chen [35] calculated the activation energy for the insertion barrier "**C**" to "**D**" with styrene as 12.30 kcal/mol. The activation with 1-octene seems to be the less favourable outcome. The metallocyclobutane intermediates are in both cases of similar thermodynamic electronic stability. The difference here is that ΔE from "**C**" to "**D**" for ethene is −4.67 kcal/mol but for 1-octene it is −6.49 kcal/mol, which could be a small driving force for 1-octene activation. The other big difference between the ethene and 1-octene routes is the dissociation of the product (styrene) to form the alkylidene species **F1** and **F4**, respectively ("**D**" to "**F**"). In the 1-octene route the energy increases with 9.52 kcal/mol (**D4**–**F4**) while the ethene route requires 15.28 kcal/mol (energy of **F1** is 22.11 kcal/mol following the ethene route), which could severely hamper the rate of activation. Thus if the substrate is changed from a C2 to a C8 alkene, deviations in the electronic profiles are observed which could have an impact on the rate of activation of the complexes. One should therefore be careful to directly apply the model with ethene as a simple substrate to systems using larger substrates like 1-octene.

The activation steps for the formation of the methylidene and heptylidene species was investigated in more detail to determine which pathway is more favourable (Fig. 8). Activation step 3 is not shown because of its similarity to activation step 4. Activation step 4 (**B** to **C4** to **F4**) is kinetically and thermodynamically more favourable than activation steps 1 (**B** to **C1** to **F1**) and 2 (**B** to **C2** to **F1**; note **F2** = **F1**). The activation energy of the rate-limiting step ("**D**" to "**E**") for heptylidene formation is 25.44 kcal/mol while methylidene formation requires more

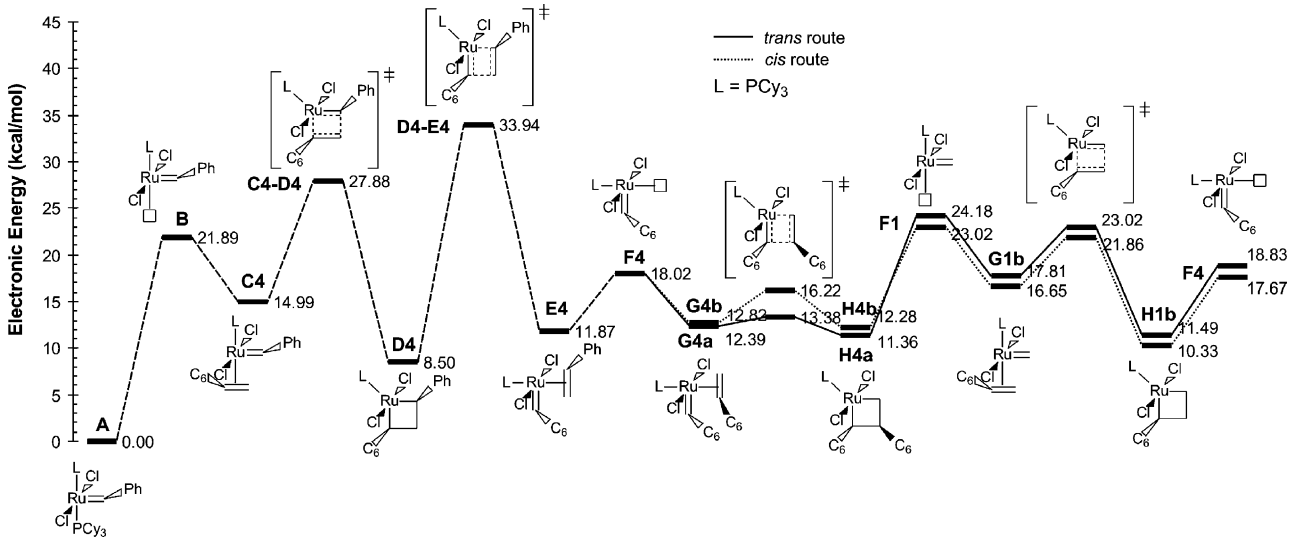

Fig. 10. Electronic energy profile of a complete pathway in the 1-octene metathesis mechanism using $RuCl_2(PCy_3)_2(=CHPh)$ (*trans* structures only are shown from **F4** to **F1**).

than 29 kcal/mol and the overall energy change from "**B**" to "**F**" is −3.87 kcal/mol and approximately 17 kcal/mol, respectively. This explains the ^{1}H NMR result, which shows the rapid formation of the heptylidene at the onset of the reaction.

The catalytic cycles using the heptylidene **F4** were further investigated; a 1-octene molecule now coordinates to the catalytically active species to yield **H4** (see Scheme 3). Stereochemically this coordination can take place in two different modes, the hexyl groups *trans* (**G4a**) and the hexyl groups *cis* (**G4b**), with their respective electronic energy profiles illustrated in Fig. 9. The two approaches give rise to transition states with different electronic energies; the *cis* mode requiring 3.40 kcal/mol and the *trans* mode only 0.99 kcal/mol. The metallacyclobutane intermediates that form (**H3a** and **H3b**) then liberates the PMPs, *trans*-7-tetradecene and *cis*-7-tetradecene, and the methylidene (**F1**). The *trans*/*cis* ratio found experimentally (Fig. 2) correlates roughly with the corresponding activation energy ratio.

Finally the completion of the catalytic cycle, **F1** to **F4**, was modelled. The complete electronic energy profile of **A** to **F4** to **F1** to **F4** is illustrated in Fig. 10. The conversion to the heptylidene (**F1**–**F4**) is thermodynamically favoured over the conversion to the methylidene (**F4**–**F1**) with changes in electronic energies of approximately −5 and 6 kcal/mol, respectively. The different energies shown in the **F1** to **F4** cycle is due to the formation of *trans*- and *cis*-7-tetradecene carried over in the mass balance used for the calculation.

4. Conclusions

Using DMol^3 density functional theory calculations we have described the 1-octene metathesis reaction by a dissociative mechanism. A deeper insight into the NMR results were gained with the use of molecular modelling, indicating that the heptylidene species is the catalytically active species that preferentially forms in the 1-octene metathesis reaction with **1**.

The DMol^3 density functional theory calculations compared very well with calculations by other authors. We also found that the same simple models that efficiently describe the metathesis of simple substrates with a methylidene type catalyst cannot be used to describe the reaction of real systems. It is clear that the mechanism of metathesis with actual catalytic systems are complex if it is done with large substrates like 1-octene and that electronic effects cannot fully account for effects that are observed like the *cis*/*trans* isomerisation of the primary metathesis product. Since this was a preliminary computational study of the complete catalytic cycle we could not make any clear conclusions regarding activity. What can be concluded is that the complete catalytic cycle with 1-octene is a very complex reaction and cannot just be considered by using a simple model. Further studies of the complete system are necessary to fully understand this mechanism.

Acknowledgements

We would like to express our gratitude towards Werner Janse van Rensburg (Sasol Technology R&D) for the valuable discussions and Andre Joubert for acquiring the NMR data. The North-West University (Potchefstroom Campus) for their financial support of our laboratory for applied molecular modelling; Sasol Technology R&D and the THRIP programme (grant #2789) of the National Research Foundation of South Africa for their financial contribution towards the studies of M.J.

References

[1] K.J. Ivin, J.C. Mol, Olefin Metathesis and Metathesis Polymerization, Academic Press, San Diego, 1997.
[2] F.Z. Dörwald, Metal Carbenes in Organic Synthesis, Wiley-VCH, 1999.
[3] A.M. Rouhi, Chem. Eng. (2002) 29.
[4] P.H. Wagner, Chem. Ind. (1992) 330.
[5] A. Fürstner, Angew. Chem. Int. Ed. 39 (2000) 3012.
[6] C. van Schalkwyk, H.C.M. Vosloo, J.A.K. du Plessis, Adv. Synth. Catal. 344 (2002) 781.
[7] M. Dinger, J. Mol, Adv. Synth. Catal. 344 (2002) 671.
[8] J. Huang, H.-J. Schanz, E.D. Stevens, S.P. Nolan, Organometallics 18 (1999) 5375.
[9] T. Weskamp, F.J. Kohl, W. Hieringer, D. Gleich, W.A. Herrmann, Angew. Chem. Int. Ed. 38 (1999) 2416.
[10] J.L. Herrisson, Y. Chauvin, Makromol. Chem. 141 (1971) 161.
[11] E.L. Dias, S.T. Nguyen, R.H. Grubbs, J. Am. Chem. Soc. 119 (1997) 3887.
[12] M. Ulman, R.H. Grubbs, Organometallics 17 (1998) 2484.
[13] M.S. Sanford, J.A. Love, R.H. Grubbs, J. Am. Chem. Soc. 123 (2001) 6543.
[14] C. Adlhart, P. Chen, J. Am. Chem. Soc. 126 (2004) 3496.
[15] M.S. Sanford, M. Ulman, R.H. Grubbs, J. Am. Chem. Soc. 123 (2001) 749.
[16] C. Adlhart, C. Hinderling, H. Baumann, P. Chen, J. Am. Chem. Soc. 122 (2000) 8204.
[17] B. Delley, J. Chem. Phys. 92 (1990) 508;
B. Delley, J. Chem. Phys. 113 (2000) 7756;
B. Delley, J. Phys. Chem. 100 (1996) 6107.
[18] http://www.accelrys.com/.
[19] J.P. Perdew, Y. Wang, Phys. Rev. B 45 (1992) 13244.
[20] B. Delley, Modern Density Functional Theory: A Tool for Chemistry, in: J.M. Seminario, P. Politzer (Eds.), Theoretical and Computational Chemistry, vol. 2, Elsevier, Amsterdam, 1995.
[21] J. Andzelm, R.D. King-Smith, G. Fitzgerald, Chem. Phys. Lett. 335 (2001) 321.
[22] W. Janse van Rensburg, C. Grové, J.P. Steynberg, K.B. Stark, J.J. Huyser, P.J. Steynberg, Organometallics 23 (2004) 1207;
W. Janse van Rensburg, P.J. Steynberg, W.H. Meyer, M.M. Kirk, G.S. Forman, J. Am. Chem. Soc. 126 (2004) 14332.
[23] G. Henkelman, H. Jonsson, J. Chem. Phys. 113 (2000) 9978.
[24] J.A. Love, M.S. Sanford, M.W. Day, R.H. Grubbs, J. Am. Chem. Soc. 125 (2003) 10103.
[25] J. Louie, R.H. Grubbs, Organometallics 21 (2002) 2153.
[26] J. Huang, E.D. Stevens, S.P. Nolan, J.L. Petersen, J. Am. Chem. Soc. 121 (1999) 2674.
[27] S. Vyboishchikov, M. Bühl, W. Thiel, Prof., Chem. Eur. J. 8 (2002) 3962.
[28] K.A. Burdett, L.D. Harris, P. Margl, B.R. Maughon, T. Mokhtar-Zadeh, P.C. Saucier, E.P. Wasserman, Organometallics 23 (2004) 2027.
[29] L. Cavallo, J. Am. Chem. Soc. 124 (2002) 8965.
[30] F. Bernardi, A. Bottoni, G.P. Miscione, Organometallics 22 (2003) 940.
[31] S. Fomine, S.M. Vargas, M.A. Tlenkopatchev, Organometallics 22 (2003) 93.
[32] C.A. Tolman, Chem. Rev. 77 (1977) 313.
[33] K.A. Bunten, L. Chen, A.L. Fernandez, A.J. Poe, Coord. Chem. Rev. 41–51 (2002) 233.
[34] S.T. Nguyen, T.M. Trnka, in: R.H. Grubbs (Ed.), Handbook of Metathesis, vol. 1, Wiley-VCH, 2003, p. 61.
[35] C. Adlhart, P. Chen, Angew. Chem. Int. Ed. 41 (2002) 4484.